

Formation of Gallium Dimers in the Intermetallic Compounds R_5Ga_3 ($R = Sc, Y, Ho, Er, Tm, Lu$). Deformation of the Mn_5Si_3 -Type Structure

Paul A. Maggard and John D. Corbett*

Department of Chemistry, Iowa State University, Ames, Iowa 50014

Received October 24, 2000

The R_5Ga_3 ($R = Sc, Y, Ho, Er, Tm, Lu$) phases were prepared by high-temperature solid-state techniques. The structure of monoclinic Sc_5Ga_3 was determined by single-crystal X-ray diffraction means ($C2/m$, No. 12, $Z = 4$, $a = 8.0793(5)$ Å, $b = 14.003(1)$ Å, $c = 5.9297(3)$ Å, $\beta = 90.994(5)^\circ$), and those of the isotypic R_5Ga_3 , $R = Y, Ho, Er, Tm, Lu$, were determined by Guinier powder diffraction. The new Sc_5Ga_3 structure is a deformation of the hexagonal Mn_5Si_3 type ($P6_3/mcm$) and contains two types of gallium dimers with $d(Ga-Ga) = 2.91$ and 3.14 Å. The closely spaced Sc1 chains in the parent Mn_5Si_3 type transform to zigzag chains in concert with displacements of the uniformly spaced gallium atoms to form dimers within distorted confacial square antiprisms of Sc. Matrix effects appear important in the different Ga_2 bond lengths. Electronic calculations reveal that the transformation from the hypothetical Mn_5Si_3 to the Sc_5Ga_3 type is aided by antibonding Ga–Ga interactions between the dimers that are pushed above E_F and Ga–Ga and Ga–Sc bonding states just below E_F that are stabilized. Sc_5Ga_3 is appropriately metallic. Except for $R = Sc, Lu$, the arc-melted R_5Ga_3 compounds above slowly transform on annealing at 1150 °C and below into tetragonal Ba_5Si_3 -type structures.

Introduction

Compounds with the Mn_5Si_3 -type structure have been sources of useful chemical instruction as well as of significant experimental errors, both deriving from a remarkable flexibility of this particular structure type to accommodate a great range of host substitutions as well as to bind diverse interstitials Z .¹ The latter variable has led to extensive studies of several families of compounds Zr_5Sb_3Z ,² Zr_5Sn_3Z ,³ Zr_5Pb_3Z ,⁴ La_5Pb_3Z ,⁵ La_5Ge_3Z ,⁶ La_5Sn_3Z ,⁷ Ae_5Pn_3Z ($Ae =$ alkaline-earth metal; $Pn =$ pnictogen),^{8–10} and R_5Pn_3Br ($R =$ rare-earth metal).¹¹ The electron-rich hosts among these can bind up to 20 different Z elements, usually a main-group element or transition metal, in an antiprismatic interstitial metal site. The B-site substitutional chemistry in these A_5B_3 compounds that has been explored includes $M_5Tr_{3-x}Sb_x$ ($M = Ti, Zr, Hf; Tr = Al, Ga$),¹² $Zr_5Ir_{3-x}T_x$ ($T = Pt$ or Os),¹³ and more recently, $Sc_5Tr_{3-x}X_x$ (for $Tr = Al, Ga; X = Sn, Sb, Te$).¹⁴ These interstitial or substitution reactions

often happen quite unexpectedly through contamination by a third element, such as from water or oxygen, and this may even lead to a unique stabilization of some ternary phases.¹ For example, $Sc_5Al_{3-x}Te_x$ is stable in this structure type for $1 > x > 0.8$, but neither binary end member, Sc_5Al_3 or Sc_5Te_3 , can be synthesized.¹⁴ Compounding these problems is the fact that many Mn_5Si_3 -type examples were identified decades ago, usually according to X-ray powder diffraction patterns, and have never been reevaluated using modern diffractometry techniques. For those wishing to make chemical sense out of this large class of compounds, it is first essential to know their compositions and structures accurately.

The R_5Ga_3 ($R =$ rare-earth element) compounds were first reported some years ago to have either the Cr_5B_3 structure type for $R = Y, La, Nd, Sm-Dy$ or the Mn_5Si_3 structure type for the smaller $R = Sc, Y, Ho-Tm, Lu$.^{15,16} However, single-crystal studies a few years ago revealed that the La, Gd , and low-temperature Y examples actually crystallize in a distorted Cr_5B_3 version, more commonly known as the Ba_5Si_3 type, whereas Guinier X-ray powder data indicated that the quenched Y, Ho , and Er members with nominal Mn_5Si_3 -type structures were irregular as well.¹⁷ The former La_5Ga_3 and both forms of Y_5Ga_3 were also found to exhibit Pauli-like magnetic susceptibilities characteristic of a metallic state. Our motivation for studying the R_5Ga_3 systems began with discrepancies evident in the volume and axial length trends across the Mn_5Si_3 -type solution series $Sc_5Ga_{3-x}(Sn, Sb, \text{ or } Te)_x$, in which sharp deviations from Vegard's law (linearity) occur, i.e., mostly a compression of the c axis of the ideal hexagonal unit cell, as x approached 0 (Sc_5Ga_3). Also, splittings of several Guinier powder-pattern lines characteristic of the Mn_5Si_3 structure were apparent in these

- (1) Corbett, J. D.; Garcia, E.; Guloy, A. M.; Hurng, W.-M.; Kwon, Y.-U.; Leon-Escamilla, E. A. *Chem. Mater.* **1998**, *10*, 2824.
- (2) Garcia, E.; Corbett, J. D. *Inorg. Chem.* **1988**, *27*, 2353.
- (3) Kwon, Y.-U.; Corbett, J. D. *Chem. Mater.* **1992**, *4*, 1348.
- (4) Kwon, Y.-U.; Corbett, J. D. *J. Alloys Compd.* **1993**, *190*, 219.
- (5) Guloy, A. M.; Corbett, J. D. *J. Solid State Chem.* **1994**, *109*, 352.
- (6) Guloy, A. M.; Corbett, J. D. *Inorg. Chem.* **1993**, *32*, 3532. Guloy, A. M.; Corbett, J. D. *Inorg. Chem.* **1996**, *35*, 4669.
- (7) Kwon, Y.-U.; Rzeznik, M. A.; Guloy, A. M.; Corbett, J. D. *Chem. Mater.* **1990**, *2*, 546.
- (8) Hurng, W.-M.; Corbett, J. D. *Chem. Mater.* **1989**, *1*, 311.
- (9) Leon-Escamilla, E. A.; Corbett, J. D. *J. Alloys Compd.* **1994**, *206*, L15.
- (10) Leon-Escamilla, E. A.; Corbett, J. D. *J. Alloys Compd.* **1998**, *265*, 104.
- (11) Jensen, E. A.; Hoistad, L. M.; Corbett, J. D. *J. Solid State Chem.* **1999**, *144*, 175.
- (12) Boller, H.; Parthé, E. *Acta Crystallogr.* **1963**, *16*, 830.
- (13) Waterstrat, R. M.; Keuntzler, R.; Muller, J. J. *Less-Common Met.* **1990**, *167*, 169.
- (14) Maggard, P. A.; Knight, D. A.; Corbett, J. D. *J. Alloys Compd.*, in press.

- (15) a) Schob, O.; Parthé, E. *Acta Crystallogr.* **1964**, *17*, 1335. (b) Palenzona, A.; Franceschi, E. *J. Less-Common Met.* **1968**, *14*, 47.
- (16) Dzyana, D. I.; Kripyakevich, P. I. *Dopov. Akad. Nauk. Ukr. RSR, Ser. A* **1969**, *31*, 247; *Khim. Khim. Tekhnol.* **1970**, *1*, 116.
- (17) Zhao, J.-T.; Corbett, J. D. *J. Alloys Compd.* **1994**, *210*, 1.

Table 1. Lattice Constants and Cell Volumes of R_5Ga_3 Phases ($C2/m$)^a

compound	<i>a</i> , Å	<i>b</i> , Å	<i>c</i> , Å	β , deg	<i>V</i> , Å ³
Sc ₅ Ga ₃	8.0793(5)	14.003(1)	5.9297(3)	90.994(5)	670.76(7)
Lu ₅ Ga ₃	8.4021(4)	14.553(9)	6.2811(5)	91.11(5)	767.87(8)
Tm ₅ Ga ₃	8.4670(8)	14.647(1)	6.3489(8)	91.28(1)	787.2(1)
Er ₅ Ga ₃	8.5081(8)	14.721(2)	6.3776(4)	91.30(1)	798.6(1)
Ho ₅ Ga ₃	8.5571(8)	14.768(1)	6.4195(8)	91.35(6)	811.0(1)
Y ₅ Ga ₃	8.616(2)	14.859(3)	6.516(2)	91.46(2)	834.0(4)

^a From Guinier powder diffraction data with Si as the internal standard, 23 °C, $\lambda = 1.54056$ Å.

regions.¹⁴ A single-crystal diffraction study of these anomalies for Sc₅Ga₃ and powder pattern examination of other R₅Ga₃ systems have illuminated the first substantive distortion of the Mn₅Si₃ structure type, and subsequent electronic band structure calculations have afforded a useful description of the bonding changes.

Experimental Section

Syntheses. Gallium (Johnson-Matthey) and the rare-earth elements Sc, Y, Ho, Er, Tm (Ames Laboratory) were used as received with stated purities greater than 99.9%. All starting materials and reaction products were handled in a helium-filled glovebox that included a built-in arc melter. About 300–350 mg of the elements necessary to give R₅Ga₃ compositions were weighed out, and the rare-earth-metal components were pelletized into 10 mm diameter disks with the aid of a hydraulic press. Gallium metal liquifies upon compression and so could not be easily pelletized. Therefore, the R pellet and the solid gallium piece were transferred to the water-cooled copper hearth, with the rare-earth metal component on top, and these were arc-melted together at 70 A for 20 s per side, with intermittent melting of a zirconium getter for oxygen. Pellet weight losses were typically 1–2% and did not affect the overall sample compositions significantly. The arc-melted pellets were then sealed into 9 mm i.d. tantalum tubing, transferred to a high-temperature vacuum furnace (Thermal Technology), annealed at 1150 °C for 2 days, and cooled to 1050 °C over 20 h. Then the power was turned off. X-ray powder patterns taken both before and after annealing typically indicated quantitative yields (>95%) and better crystallinity after annealing. However, the annealing and cooling procedure resulted in partial (≥25%) conversion of the (Y, Ho, Er, Tm)₅Ga₃ compounds to the Ba₅Si₃ type, which confirmed an earlier report,¹⁷ while (Sc, Lu)₅Ga₃ remained the unchanged (nominal) Mn₅Si₃ type.

Powder X-ray Diffraction. The powder diffraction patterns of the samples were obtained with the aid of Enraf-Nonius Guinier cameras and monochromatic Cu K α_1 radiation. The brittle samples were powdered, mixed with standard silicon (NIST) as a calibrant, and placed between two strips of cellophane tape on a frame that was mounted on the camera rotation motor. Refined lattice parameters for all six Sc₅Ga₃-type phases are given in Table 1, arranged in order of increasing unit cell volume.

Single-Crystal X-ray Diffraction. Shiny black single crystals were selected from a reaction loaded as Sc₅Ga₃ and were sealed inside 0.3 mm glass capillaries. Crystal qualities were inspected with Laue photographs, and the best crystal was selected for data collection on a Bruker CCD diffractometer operating at room temperature with Mo K α radiation. Three sets of 30 frames with 15 s exposures were used to determine provisional lattice constants and the crystal system. The lattice constants, angles, and absences suggested a C-centered monoclinic space group with $\beta \approx 91.0^\circ$, which is a small angular distortion of the C-centered orthorhombic equivalent to the parent hexagonal cell of Mn₅Si₃ that is obtained by the transformation $[a, b, c]_{\text{hex}}[1/2, -1/2, 0; 1/2, 1/2, 0; 0, 0, 1] = [a, b, c]_{\text{ortho}}$. One-half a sphere of reflections was collected to $2\theta \approx 56^\circ$, utilizing 30 s frame exposures. The reflections, when integrated and filtered with SAINTPLUS,¹⁸ yielded 1719 allowed reflections of which 619 were unique and observed ($I > 2\sigma_I$). An absorption correction was applied with the package program SAD-

Table 2. Selected Crystal and Refinement Data for Sc₅Ga₃^a

fw	867.92
space group, <i>Z</i>	$C2/m$ (No. 12), 4
d_{calc} , g cm ⁻³	4.285
μ (Mo K α), mm ⁻¹	16.412
data/restraints/params	619/0/42
final R1, wR2 ^a [$I > 2\sigma(I)$]	0.0637, 0.1720
largest diff peak and hole, e Å ⁻³	1.946 (0.96 Å from Ga2), -1.905

^a $R1 = \sum||F_o| - |F_c||/\sum|F_o|$; $wR2 = \{\sum[w(F_o^2 - F_c^2)^2]/\sum[w(F_o^2)^2]\}^{1/2}$, $w = \sigma_F^{-2}$.

Table 3. Atomic Coordinates and Equivalent Isotropic Displacement Parameters (Å² × 10³) for Sc₅Ga₃

atom	Wyckoff	<i>x</i>	<i>y</i>	<i>z</i>	<i>U</i> (eq) ^a
Ga1	4 <i>m</i>	0.0971(3)	0	0.7094(4)	16(1)
Ga2	8 1	0.2000(2)	0.2998(1)	0.7717(3)	19(1)
Sc1	4 2	0	0.1777(3)	0.5	15(1)
Sc2	8 1	0.3785(3)	0.1205(2)	0.7551(4)	15(1)
Sc3	4 <i>m</i>	0.2628(5)	0	0.2570(6)	16(1)
Sc4	4 2	0	0.1551(3)	0	16(1)

^a *U*(eq) is defined as one-third of the trace of the orthogonalized U_{ij} tensor.

ABS,¹⁹ and structural models were obtained and refined with the SHELXTL program.²⁰ Intensity statistics were ambiguous, but refinement tests of all three possible space groups $C2$, Cm , and $C2/m$ produced the lowest residuals and smallest positional errors for $C2/m$. Some data collection and refinement parameters are given in Table 2. The refinement converged at $R1/wR2 = 0.064/0.172$, using a full-matrix least-squares refinement on F^2 and a reflection:variable ratio of 14.7:1. The positional and isotropic-equivalent displacement parameters for Sc₅Ga₃ are given in Table 3. Additional data collection, refinement, and anisotropic displacement parameters and all near-neighbor interatomic distances are given in the Supporting Information. The distances were calculated utilizing the more accurate lattice parameters determined with the aid of Guinier powder diffraction. The Supporting Information material and the F_o/F_c listing are available from J.D.C.

Band Calculations. Extended Hückel band calculations were carried out within the tight-binding approximation²¹ for the real and for the hypothetical undistorted (Mn₅Si₃-type) structure of Sc₅Ga₃ at 150 k-points spread out over the irreducible wedge. H_{ii} parameters employed were those values obtained by iteration to charge consistency for the full structure (eV): Sc 4s, -7.33; Sc 4p, -3.53; Sc 3d, -6.89; Ga 4s, -14.58; Ga 4p, -6.75.

Results and Discussion

Structural Description. A near-[001] view of the Sc₅Ga₃ structure is given in Figure 1, with selected Sc–Sc and Ga–Ga distances labeled in Å. The complex scandium network (black atoms) is constructed from four symmetry-inequivalent positions. The Sc2 and Sc3 atoms define distorted chains of confacial trigonal antiprisms along $(1/2, 0, z)$, $(0, 1/2, z)$, clear remnants of Mn2 in the Mn₅Si₃ structure when viewed in terms of the larger C-centered orthorhombic cell. The faces are nearly equilateral with side lengths (~ 3.36 Å) that differ by 0.018(9) Å, whereas the interatomic distances between the two faces range from 3.48 to 3.64 Å. The Sc1 and Sc4 atoms (the former linear chain of Mn1) describe a zigzag chain spaced at 2.98 Å along *c*, and these serve to edge-bridge three antiprismatic Sc chains at 3.36 to 3.60 Å. It should be noted here that to aid in the visualization of the 3D structure, some arbitrary distance cutoff limits (supported by band calculation results) have been used in drawing some of the contacts.

(19) Blessing, R. H. *Acta Crystallogr.* **1995**, *A51*, 33.

(20) SHELXTL; Bruker, AXS, Inc.: Madison, WI, 1997.

(21) Hoffmann, R. *J. Chem. Phys.* **1963**, *39*, 1397. Whangbo, M.; Hoffmann, R. *J. Am. Chem. Soc.* **1978**, *100*, 6093.

(18) SAINTPLUS; Bruker AXS, Inc.: Madison, WI, 1996.

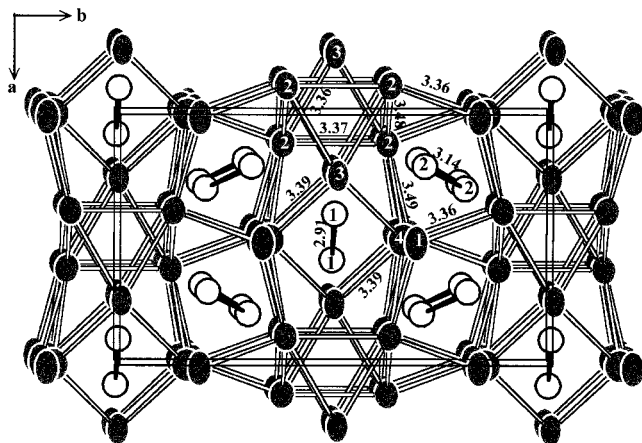


Figure 1. Near-[001] view of the monoclinic Sc_5Ga_3 structure with selected Sc–Sc and Ga–Ga distances labeled in units of Å. Black atoms represent scandium, and white atoms represent gallium. The symmetry elements are a vertical mirror plane at $y = 0, 1/2$ and centers of symmetry in the dimers and confacial antiprims ($0, 1/2, 0$, etc.) (99.9% probability displacements appear in all figures).

Two types of centric gallium dimers (open ellipsoids) with bond distances of 2.91 Å (Ga1–Ga1) and 3.14 Å (Ga2–Ga2) are located in cavities defined by portions of two antiprismatic and two zigzag chains of scandium. The D_{2h} environment around Ga1–Ga1 is better seen in the [010] section around $y = 1/2$ in Figure 2a. The gallium atoms are each located in distorted trigonal prisms of Sc1,2,4 that share Sc1–Sc1 edges. (Each trigonal prism shares edges with two other trigonal prisms down c that are formed by the Sc1, Sc4 zigzag chains.) Distances from Ga1 to the vertexes of the surrounding Sc trigonal prisms are quite similar, 2.85–2.89 Å, and additional Sc3 atoms above their rectangular faces (1–1–4–4 and 1–1–2–2) give each Ga1 atom two additional neighbors at 2.91 and 3.02 Å (dashed) for a total coordination of eight Sc. Note that the side edges of the prisms in this view vary greatly, 3.37 Å for Sc2–Sc2, 4.35 Å for Sc4–Sc4, and 4.97 Å for Sc1–Sc1; that is, their basal faces are distinctly nonparallel. (The trigonal prism edges surrounding (Ga1)₂ exist in Figure 1 only as the long unmarked horizontal Sc1–Sc1 and Sc4–Sc4 connections across the central square around $1/2, 1/2, 1/2$ plus the Sc2–Sc2 edges.) Because of the distortions, it is probably more useful to describe the Ga1–Ga1 dimer as bonded through the more open Sc3–Sc1–Sc3–Sc1 face common to two distorted, confacial square antiprims (3, 3, 2, 4).

The situation around (Ga2)₂, within a similar square unit in Figure 1, is necessarily different because (Ga2)₂ has been rotated by $\sim 60^\circ$ from that of (Ga1)₂ just described and possesses only a center of symmetry. In Figure 2b, each Ga2 now has six rather than three independent distances to the trigonal prismatic scandium atoms at 2.83–2.95 Å (not labeled), very similar to the closest six Sc atoms about Ga1. The face-capping Sc2 atoms here (dashed) are at 2.90 and 3.10 Å, the latter to the upper Sc2 being 0.08 Å longer than in Figure 2a. The similar distances for the Ga2-centered trigonal prism edges are 3.36 Å for Sc2–Sc3, 4.52 Å for Sc1–Sc1, and 4.84 Å for Sc4–Sc4. The crux of the difference in the two dimers seems to lie in the intervening distorted squares. The Ga1–Ga1 bond lies between two Sc1 atoms separated by 4.97 Å, while that for Ga2–Ga2 occurs between two Sc4 atoms 4.84 Å apart, 0.14 Å less. (The other Sc3–Sc3 and Sc4–Sc4 diagonals on the common waist are longer, 5.17 and 5.11 Å, respectively.) With very comparable Ga–Sc neighbor distances about Ga1 and Ga2 dimers (each lies across a center of symmetry), the “squeeze” of the two Sc4

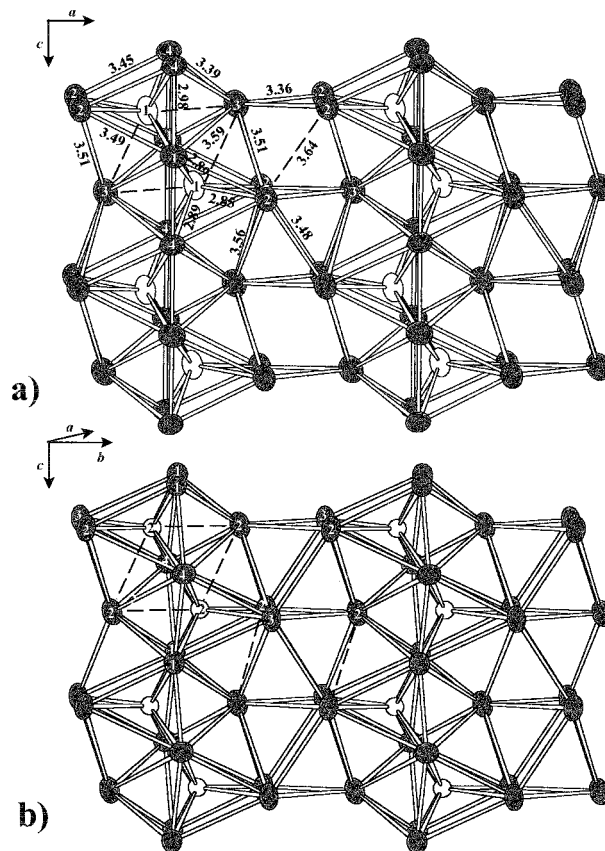


Figure 2. (a) A [010] section of the structure of Sc_5Ga_3 , showing the pairs of augmented edge-sharing scandium trigonal prisms about (Ga1)₂ and the open Sc1–3–1–3 face through which the dimer extends. (The Sc3 atoms lie on a mirror plane normal to the view.) (b) Similar environment about the longer (Ga2)₂. The reduced centrosymmetric symmetry (compare Figure 1) splits nearly all dimensions of and within the trigonal prisms by ~ 0.1 – 0.2 Å (not marked) except for the fixed $d(\text{Sc1}–\text{Sc4}) = 2.98$ Å. The atom colorings are as in Figure 1.

Table 4. Atomic Displacements (Å) in Sc_5Ga_3 from the Ideal C-Centered Orthorhombic Equivalent of the Mn_5Si_3 -Type Structure

atom type ^a	x	y	z
Ga1	−0.088	0	−0.241
Ga2	+0.032	+0.07	+0.129
Sc1	0	+0.154	0
Sc2	−0.036	+0.042	+0.030
Sc3	0	0	0
Sc4	0	−0.163	0

^a In the hexagonal setting there are only three unique atom positions: Sc1 = Sc4 = (Sc1)_{hex} ($1/3, 2/3, 0$); Sc2 = Sc3 = (Sc2)_{hex} ($x, 0, 1/4$); Ga1 = Ga2 = (Ga)_{hex} ($x, 0, 1/4$).

appears to force the elongation of the latter, that is, a matrix effect. The interdimer separation between the (Ga2)₂ units is correspondingly a little less than between (Ga1)₂, 3.6 vs 3.8 Å. The distortion about the second dimer also opens up the top basal face of the trigonal prism by 0.15–0.23 Å.

The Sc_5Ga_3 structure is the result of a complex 3-D network adjustments necessary to accommodate the dimers, the formation of which seems to be electronically driven (below). Numerical displacements of the various atoms from those in the equivalent C-centered orthorhombic Mn_5Si_3 -type structure are listed in Table 4. The linear M1 metal chain atoms in the parent are displaced alternately along \vec{b} by ~ 0.15 – 0.16 Å (Figure 1). Naturally Ga1 and Ga2 undergo substantial changes along z , moving toward a like atom, more so for Ga1 in the shorter dimer. The combined displacements of Sc1, Sc4, Ga1, and Ga2

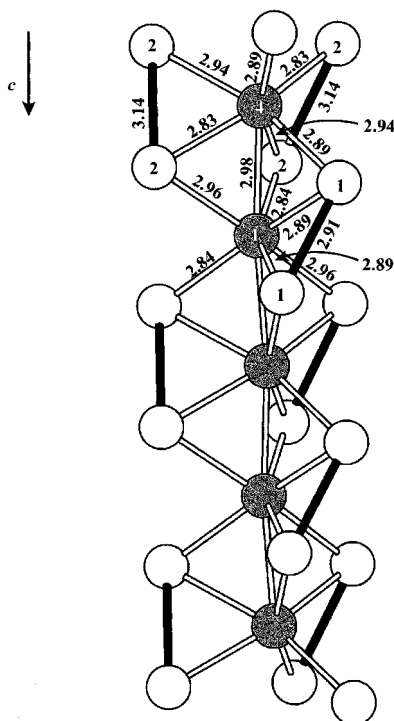


Figure 3. Section of the Sc_5Ga_3 structure along \bar{c} around the Sc1–Sc4 (black) zigzag chain with the surrounding $(\text{Ga}1)_2$ and $(\text{Ga}2)_2$ dimers (black bonds). The latter atoms define octahedra about the Sc atoms (compare with Figure 2).

are better appreciated in Figure 3, which shows the zigzag chain of Sc1,4 atoms running vertically. Each of these is surrounded by a distorted gallium octahedron, either two Ga2 dimers and the ends of two Ga1 dimers (Sc4) or the ends of four Ga2 dimers and one Ga1 dimer (Sc1), all at 2.83–2.96 Å. The chain atoms Sc1 and Sc4 move orthogonally away from the nearest dimer formation. This alternation of two $(\text{Ga}2)_2$ with one $(\text{Ga}1)_2$ dimer along z is now more evident in the projection in Figure 1 as the three columns of dimers that surround the Sc1, Sc4 “maypole” at $1/2, \sim 0.34, z$, etc. Referring back to Figure 2, this distortion of the scandium zigzag chain lengthens the edges of the scandium trigonal prisms through which the gallium atoms bond.

Isostructural Compounds. Previous research demonstrated that R_5Ga_3 compounds containing rare-earth metals larger than holmium form in either the W_5Si_3 type (Ce, Pr) or the Ba_5Si_3 type (La, Nd, Sm, Gd, Tb, Dy).^{15–17} Some experimental evidence for the heavier rare-earth gallides having a distorted Mn_5Si_3 structure was noted before¹⁷ but not investigated farther. It has now proved possible to prepare isotypic heavier rare-earth analogues of the monoclinic Sc_5Ga_3 (Table 1), the cell dimensions and presumably the gallium dimer distances increasing for larger R. The R_5Ga_3 phases for R = Ho–Tm obtained by arc-melting appear metastable at 1050–950 °C or below as they (only) partially transform to a Ba_5Si_3 version on cooling (see Experimental Section for details).

Band Calculations. Extended Hückel (tight-binding) calculations seemed necessary to understand more about the electronic structures and the distortion of the ideal Mn_5Si_3 -type structure. Figure 4 shows the total densities of states (DOS) on the same scale for both the real Sc_5Ga_3 (part I of Figure 4) and a hypothetical undistorted Mn_5Si_3 type (part II of Figure 4) modeled dimensionally according to the unsplit lines of the basic powder pattern. (The c dimension estimated by extrapolation of lattice constants for substitutional solutions would actually be somewhat larger.¹⁴) Partial contributions of the scandium

Table 5. Interatomic Distances (Å) and Corresponding Pairwise Overlap Populations (OP) in Sc_5Ga_3

atom	atom	distance	OP	atom	atom	distance	OP
Ga2	Sc3	2.827(2)	0.390	Sc1	Sc4	2.983(2)	0.148
Ga2	Sc2	2.829(2)	0.387	Sc2	Sc3	3.355(5)	0.094
Ga1	Sc2	2.847(4)	0.376	Sc2	Sc2	3.373(7)	0.090
Ga2	Sc1	2.837(3)	0.340	Sc2	Sc2	3.478(6)	0.066
Ga2	Sc4	2.829(2)	0.313	Sc2	Sc3	3.514(5)	0.062
Ga1	Sc4	2.894(4)	0.313	Sc1	Sc2	3.362(5)	0.061
Ga2	Sc2	2.905(4)	0.288	Sc3	Sc4	3.388(5)	0.055
Ga1	Sc3	2.920(6)	0.264	Sc2	Sc3	3.564(5)	0.053
Ga2	Sc1	2.955(2)	0.264	Sc2	Sc2	3.633(6)	0.046
Ga1	Sc1	2.886(4)	0.255	Sc1	Sc2	3.488(4)	0.040
Ga2	Sc4	2.937(4)	0.238	Sc2	Sc4	3.452(4)	0.038
Ga1	Sc3	3.023(6)	0.220	Sc2	Sc4	3.593(5)	0.021
Ga2	Sc2	3.100(4)	0.187	Sc1	Sc3	3.594(5)	0.019
Ga2	Sc2	3.369(4)	0.097				
Ga1	Sc3	3.495(5)	0.061				
Ga1	Ga1	2.913(5)	0.363				
Ga2	Ga2	3.140(4)	0.224				

and gallium orbitals are projected out in both. The Fermi level cuts through a large conduction band composed primarily of scandium orbitals with small gallium contributions near E_F , particularly in the real structure. The two DOS are fairly similar in major features except for a divergence of both Sc and Ga contributions from just below E_F on distortion, which have to do with the electronic nature of the distortion. The results are clearly consistent with the observed resistivity ($\sim 30 \mu\Omega \text{ cm}$ at 290 K, with $0.13\% \text{ K}^{-1}$) and temperature-independent Pauli-like paramagnetic susceptibility of Sc_5Ga_3 ($\chi_M(\text{corr}) = 6.3 \times 10^{-4} \text{ emu mol}^{-1}$ between 6 and 290 K).¹⁴

The corresponding crystal orbital overlap population (COOP) curves for the Sc–Sc, Sc–Ga, and Ga–Ga interactions in the real and model structures are drawn on the same scale in Figure 5. The Fermi level passes through the middle of strongly bonding Sc–Sc interactions and, as usual,^{22,23} leaves many of the bonding scandium states empty in both structures, while the Sc–Ga bonding interactions are more nearly optimized in the two structures. Differences between these alternatives are most conspicuous and important in the Ga–Ga COOP data, wherein the large antibonding spike near E_F in the undistorted structure (part II of Figure 4) broadens, decreases in amplitude by over 50%, and splits into two distinct peaks for the two gallium dimers. The former characteristic arises from closed-shell interactions in part II between nominal isolated Ga^{5-} units at $\sim 3.5 \text{ Å}$, and which the segregation into dimers splits into lower-lying inter- and higher-lying intradimer antibonding states. The splitting is larger with the greater displacement of Ga1 to form the shorter dimer, which pushes more states above E_F (not shown). The lower maximum in the Ga–Ga antibonding pair near E_F originates with the greater interdimer separation between $(\text{Ga}1)_2$ (3.8 Å), whereas the higher arises from the shorter interdimer $(\text{Ga}2)_2$ separation (3.6 Å) for which a significant number of states are emptied. Thus, some Ga–Ga antibonding levels, i.e., electron holes, lie above E_F and drive the dimer formation, sort of a Peierls distortion. Bonding Sc–Ga states just below E_F in part II of Figure 4 are also lowered by the distortion (Figure 5).

The complex 3-D structure of Sc_5Ga_3 provides a wide variety of distances and apparent bond strengths. To help clarify these, the atom pairs and distances are listed in Table 5 in descending order of pairwise overlap populations ($\text{OP} \approx \text{bond strength}$). The Sc–Ga overlap populations decrease fairly regularly with

(22) Maggard, P. A.; Corbett, J. D. *J. Am. Chem. Soc.* **2000**, *122*, 838.

(23) Maggard, P. A.; Corbett, J. D. *Inorg. Chem.* **1998**, *37*, 814.

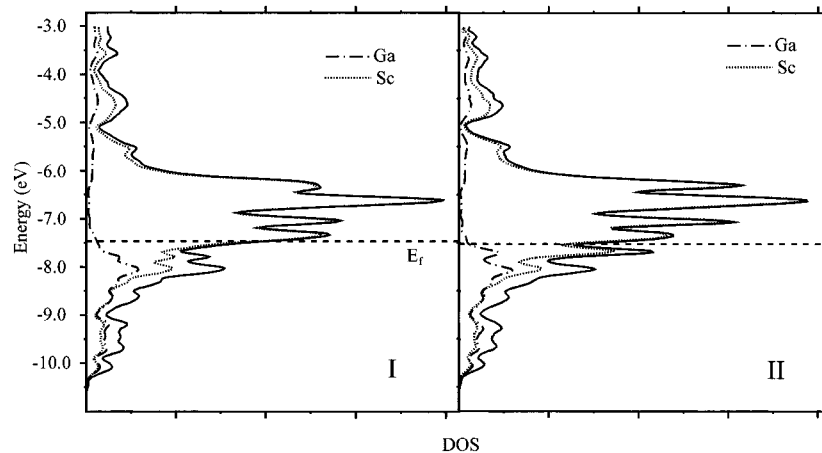


Figure 4. Total densities of states (DOS) for the real Sc_5Ga_3 structure (I) and for the undistorted Mn_5Si_3 -type model (II). The total gallium and scandium orbital contributions are projected out in each. The Fermi levels are marked by dashed lines.

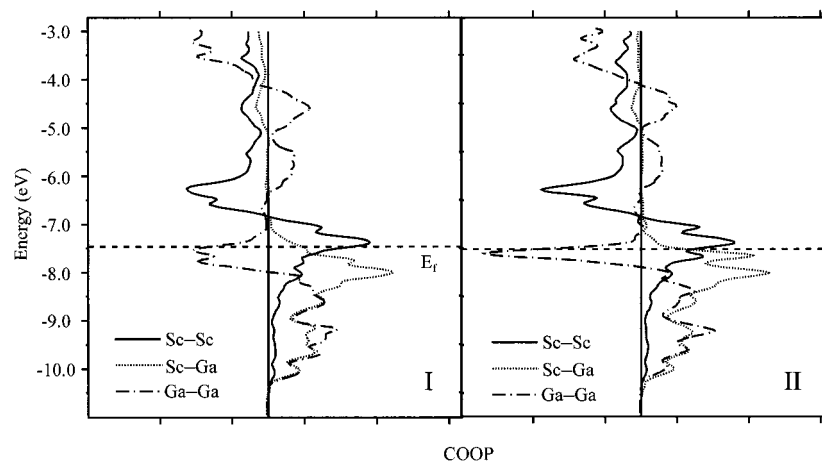


Figure 5. Crystal orbital overlap population (COOP) curves for total Sc–Sc, Sc–Ga, and Ga–Ga interactions in the real Sc_5Ga_3 structure (I) and in the undistorted Mn_5Si_3 -type model (II). Note the displacement of bonding features just below E_F on distortion to lower energies or above E_F .

increasing distances over a range 0.390–0.061 for 2.83–3.49 Å, a “normal” behavior. (The Hamilton populations will not be very different in view of the similar H_{ii} values for Sc 3d and Ga 4p.²⁴) The most obvious exception is Ga1–Sc1 with a 0.255 OP, fairly low on the list for a distance of 2.89 Å. This Sc1 sits above and below the center of the Ga1–Ga1 bond, more in the π region. The corresponding $d(\text{Ga}2\text{–Sc}4)$ above and below the longer dimer is 2.83 Å (more crowded) and has a larger OP, 0.313. Other structural situations have shown that distances alone may be poor measures of bond populations and, presumably, of strengths.²³ In the Sc–Sc metal framework, the largest OP, 0.148, goes with the Sc1–Sc4 repeat in the zigzag chain at 2.98 Å. The next larger Sc–Sc OP’s, ~ 0.09 , are within the scandium triangular faces in the ab plane, Sc2–Sc3 and Sc2–Sc2 at 3.36 and 3.37 Å, that generate the antiprismatic chain down c . The remaining Sc–Sc contacts are mostly ≥ 3.4 Å with fairly small OP’s, ≤ 0.06 , which makes it difficult to outline specific trends. As expected, the shorter (Ga1)₂ has the larger OP, 0.363, vs 0.224 for (Ga2)₂. The most reduced scandium atoms lie nearer the Ga–Ga dimers, which were partially oxidized in the distortion.

General Discussion

More general and useful considerations of the structures and their electronics among this collection of 5–3 compounds with

fairly large electronegativity differences are also possible. Tests of the electron-poor or -deficient regimes with triels (Tr = Ga, In, Tl) are especially severe because of the extreme negative oxidation states that would be required for the formation of formal closed-shell (Zintl) phases. The R_5Tr_3 compositions with Mn_5Si_3 -type structures have always been interesting because the triel elements are isolated here. These phases have accordingly been considered as possible closed-shell Zintl phases with electronic balance between R^{3+} and Tr^{5-} oxidation states, although the latter seems quite extreme and improbable. (But we now know that the Mn_5Si_3 structures reported for Ho–Lu, Y, and Sc gallides were in error because of inadequate powder pattern resolution or care.) The alternatives in such extreme circumstances are either to delocalize some of the high electron concentration on the anions into a conduction band (as well as into polar-covalent R–Tr bonds, which does not change the oxidation state) or to transform into a structure with smaller anion charge requirements, e.g., the Cr_5B_3 type with an anionic constitution that gives oxidation-state limits of $(\text{Tr}_2^{8-})(\text{Tr}^{5-})$ and two formally excess electrons. This structure is known for gallides of several earlier elements in the lanthanide series, La–Dy generally and Y, and these are in any case metallic with the distorted Ba_5Si_3 structure version of the Cr_5B_3 type that is common with large cations and small anions.¹⁷ The present Sc_5Ga_3 -type examples represent a still greater perturbation of the anion structure. Even more electron-deficient Cr_5B_3 versions are also known for Ca_5Ga_3 and Sm_5Ga_3 , both of which are

(24) Glassey, W. V.; Hoffmann, R. *J. Chem. Phys.* **2000**, *113*, 1698.

metallic, and the Ga–Ga distances therein are notably short, 2.493(1) and 2.658(4) Å, respectively, evidently because of greater loss of what could be described as higher lying (π^*) electrons.²⁵

The new Sc_5Ga_3 structure (and those for $R = \text{Ho, Er, Tm, Lu, Y}$ as well) present an alternative, with lessened electron requirements for the anions via the formation of two (nominal) Ga_2^{8-} dimers and three excess electrons formally. The structures at the melting points could well be the higher symmetry Mn_5Si_3 type ($P6_3/mcm$), which undergo probable second-order transitions on cooling to the Sc_5Ga_3 type with only dimers. Even so, the observed result is still metallic, and more of an intermetallic in characteristics than the valence phase implied by the extreme charge distribution cited. Among the known $R_5\text{Ga}_3$ prospects, the scandium compound probably has the lowest lying conduction band because of the high charge-to-radius ratio of the cations. We surmise that this drives the formation of only dimers, as opposed to the Cr_5B_3 version, by delocalization of more electrons. The same appears to apply to Lu_5Ga_3 , but with the larger and more electropositive Dy, Ho, Er, Y, the gallium dimers would presumably be longer and less stable and their Sc_5Ga_3 -type structures transform (remarkably slowly) into more stable Cr_5B_3 (Ba_5Si_3) versions. The delocalization of dimer π^* states is also known to be important in the tetrel Cr_5B_3 analogues A_5Tt_3 when A is a dipositive cation Ca–Ba plus Sm and Tt is Si–Pb. These phases are metallic for both the potentially valence-precise binaries and the oxidized $\text{A}_5\text{Tr}_3\text{Z}$ for $Z = \text{H,}$

F, and the dimers in the latter appear to be appropriately shorter.²⁶ Those in Ca_5Ga_3 and Ca_5Zn_3 are even shorter and more electron-deficient.

Conclusions

A series of isostructural compounds $R_5\text{Ga}_3$ ($R = \text{Sc, Y, Ho, Er, Tm, Lu}$) are shown to have a new distorted version of the familiar Mn_5Si_3 structure type. Structural features of the new Sc_5Ga_3 type include trigonal antiprismatic chains of Sc packed into a nearly hexagonal arrangement, each antiprism having six connections to closely spaced scandium zigzag chains that enclose two types of gallium dimers of different lengths. The gallium environments are distorted confacial square antiprisms of scandium that share edges down the c axis. The new Sc_5Ga_3 is metallic. Electronic calculations reveal that the distortion and formation of Ga_2 anions allows (a) significant displacement of antibonding dimer levels to above E_F and (b) appreciable lowering of Ga–Ga and Ga–Sc states just below E_F .

Acknowledgment. This work was supported by the National Science Foundation, Solid State Chemistry, via Grant DMR-9809850, and was carried out in the facilities of Ames Laboratory, U.S. Department of Energy.

Supporting Information Available: Tables of additional crystallographic and refinement parameters, and a complete listing of nearest-neighbor distances. This material is available free of charge via the Internet at <http://pubs.acs.org>.

IC0011720

(25) Leon-Escamilla, E. A.; Corbett, J. D. *J. Solid State Chem.*, submitted.

(26) Leon-Escamilla, E. A.; Corbett, J. D. *Inorg. Chem.*, in press.